Regulatory Mechanisms in Biosystems

ISSN 2519-8521 (Print)
ISSN 2520-2588 (Online)
Regul. Mech. Biosyst.

Histological investigation for the effect of botulinum toxin B inoculation in the gluteal group muscles of the thigh on the femoral bone of albino rabbits

S. M. Abdulateef, R. H. Thamer, A. K. Obayes

Al-Nahrain University, Baghdad, Iraq
Tikrit University, Tikrit, Iraq
University of Kirkuk, Kirkuk, Iraq

Article info
Received 09.03.2025
Received in revised form 18.04.2025
Accepted 14.05.2025

College of Sciences, Al-Nahrain University, Baghdad, Iraq. E-mail: safa.mujahed@nahrainuniv.edu.iq

College of Pharmacy, Tikrit University, Tikrit, Iraq. E-mail: reham_h_th@tu.edu.iq

Department of Biology, College of Education for Women, University of Kirkuk, Kirkuk, Iraq. E-mail: alikh@uokirkuk.edu.iq

Abdulateef, S. M., Thamer, R. H., & Obayes, A. K. (2025). Histological investigation for the effect of botulinum toxin B inoculation in the gluteal group muscles of the thigh on the femoral bone of albino rabbits. Regulatory Mechanisms in Biosystems, 16(2), e25083. doi:10.15421/0225083

Botulinum toxin B is an attenuated toxin produced by the bacterium *Clostridium botulinum* used in non-surgical cosmetic operations and for correcting skin wrinkles. This article was designed to describe the effect of denervated hind limb skeletal muscle impact on the femur bone of albino rabbits. Twenty-five male animals were enrolled in the five study groups. Five rabbits served as the control group, were given only distilled water and sacrificed at the end of the study for histological study. The remaining 20 rabbits were inoculated with a single dosage of botulinum toxin B (8 IU) between the gluteal muscle group and the biceps femoris muscle of the thigh, and each group of five was sacrificed sequentially on day 10, day 15, day 30, and day 45 after the inoculation. Samples of femur bone were removed from the dissected animals. The microscopic examination of femur bone sections of the experimental 1st group showed an irregular endosteum border and narrowed bone collar. Animals from the experimental 2nd group showed remnant lacunae of hyaline cartilage and atrophied osteocytes. In the experimental 3rd group, results showed increased cavities within the bone matrix. In the experimental 4th group, the microscopic examination revealed the diminished periosteal membrane to the endosteum, atrophied lacunae, surrounded with irregular periosteum. The femoral bone displayed numerous histological changes due to the flaccid paralysis of the gluteal group muscles (disused muscles of the hind limb) of the thigh caused by a single botulinum toxin B dose.

Keywords: botulinum toxin B; femur bone; gluteal group muscles; inoculation; periosteum.

Introduction

Bone is a unique type of connective tissue that contains 35% organic minerals and 65% inorganic proteins (Bianco, 2020). Bone undergoes ongoing resorption, remodeling, and cyclic creation (Vieira et al., 2015). The periosteum, endosteum, bone marrow, and calcified bone are strongly innervated and vascularized parts of the bone (Liu et al., 2023). The central nervous system could induce changes in bone mass (Kelly and others, 2020). Carina et al. (2020), stated that muscle contraction loading is essential for preserving appropriate bone homeostasis. Bartl et al. (2023) stated that disused skeletal muscle is a significant risk factor for developing secondary bone osteoporosis. Induced secondary osteoporosis immobility due to motor neuron diseases and extended bed rest is another factor (Brent, 2021).

Globally, cosmetic surgery procedures are rising dramatically (Griffiths & Mullock, 2018). The primary objective of cosmetic surgery is to improve a person's look (Atiyeh et al., 2020). Botulinum toxin (botox) is used in non-surgery facial cosmetics to improve facial wrinkles through skin regeneration and reshape the appearance of the lower face and neck-shoulder (Fadila et al., 2016; Park et al., 2021). Botulinum toxin is an attenuate neurotoxin produced by *Clostridium botulinum* anaerobic bacteria, inhibiting the secretion of acetylcholine at the neuromuscular junction of striated muscles, resulting in short-term flaccid paralysis (Ahsanuddin et al., 2021). In 2018, over 7 million cosmetic procedures were performed in the USA using botulinum toxin treatment (Brown & Teller, 2022). Adverse side effects of botulinum toxin occur, depending on the injection site, such as blurred vision after ptosis surgery, dysphagia, and muscular weakness (Kim et al., 2023). Botulinum toxin affects the masseter muscle, causing a temporal change in the bite force (Owen et al., 2022).

Chappard et al. (2001) were the first to study the bone loss in hind limbs of rats due to flaccid paralysis induced by BTX injection. However, some studies are focused on the side effects that could affect bone homeostasis (Al-Bari et al., 2022). Muscle atrophy affects the growth and remodeling of bones (Warner et al., 2006). Spinal cord injury (SCI) induces muscle atrophy and bone loss. (Lanyon, 1996). Post-SCI osteoporosis has a complex pathophysiology; however, one of the main factors responsible for bone demineralization is the reduction of mechanical load (Kingery, 2003). Many experimental crushed nerve studies were done in animal models (Zeng et al., 1996). This study aimed to identify a histopathological defect in the rat femur bone caused by a paralyzed sciatic nerve (Yevchuk et al., 2024). The current study was designed to demonstrate histological investigation of the effect of flaccid paralysis of the hind limb induced with botulinum toxin B inoculation in the gluteal group muscle of the thigh on the femur bone in albino rabbits.

Matherials and methods

From October 2024 to January 2025, the entire experiment decribed in the present article was carried out in the surgical lab of Tikrit University's Veterinary Medicine College.

The experiment involved twenty-five male rabbits weighing between 1100 and 1200 grams, ages 12 to 13 months. The rabbits were housed in steel cages measuring 1.250 × 0.5 ×0.5 meters, and they were given food and water prior to the experiment. The rabbits survived under suitable environmental conditions of 21 to 25 °C, free access to food and water with cleaning cycles.

The study was designed to elucidate the effect of denervated gluteal group muscles of the thigh (induced by inoculation of botulinum toxin B) on the femoral bone of albino rabbits. The biceps femoris muscle of the hind limb was inoculated with a single dose 8 IU of botulinum toxin B (botulinum toxin type B 2500 IU vial/Myobloc), which is used in treating cervical dystonia. Injectable solution from Solstice Neurosciences, Inc (San Francisco, USA) was administered using a 25 gauge syringe. A 1.0 cm needle insulated the required botulinum toxin B injectable solution (Zhou et al., 2020). The tested animals were subdivided into four groups of five rabbits each plus

control; 1st group was sacrificed after 10 days of inoculation; 2nd group: sacrificed after 15 days of inoculation; 3rd group: sacrificed after 30 days of inoculation; and 4th group: sacrifiecd after 45 days of inoculation, and the fifth group were control received nothing other than distilled water.

All animals were kept until their end period and then killed using extensive dose inhalation of chloroform vapors inside a sealed glass container. All samples from the study and control groups were taken and fixed with 10% neutral buffer formalin for 48 h, followed by decalcification in acetic acid and nitric acid for one week, and cut into the smallest possible size (Alkhafaji et al., 2024; Ali et al., 2024). The decalcified bone tissue samples of the femur bone were prepared for histological technique, followed by transfer through serial graded ethanol from 70%, 80%, 90%, and 100%, then clearing by xylene and embedded in paraffin wax at 60 °C (Nichat et al., 2024; Ajitha et al., 2024). Blocking of the samples was done, and the sectioning was performed with a 5 µm thickness using a rotary microtome (Devadze et al., 2024). After staining with hematoxylin and eosin and Masson's trichrome dyes, tissue sections were mounted on the slides using dibutyl phthalate in xylene (DPX) and covered by cover slides. The slides were examined using a light microscope and photographed by a manipulated camera prepared for this purpose.

Results

The slides of the control group rabbit femur bones display compact bone osteocytes situated within lacunae surrounded by Haversian canals covered by periosteum, which has two layers, the fibrous outer layer and osteogenic inner layer, the endosteum covered the inner face of compact bone from bone marrow (Fig. 1).

In group 1 the bony matrix was surrounded by periosteum; the outer layer was fibrous collagen bundles, and many osteoblasts occupied the inner surface. Certain osteocytes were also inside lacunae, the irregular endosteum adjacent to the bone marrow (Fig. 2i). The slide shows that the periosteum is devoid of the osteogenic layer, there is an aggregate of cellular debris within the sinus beneath the endosteum, a decreased amount of collagen bundles, atrophied osteocytes and delicate connective tissue in endosteum (Fig. 2ii).

The results for group 2 display narrowed bone collar and many lacunae, primarily devoid of osteocytes. The outer border of the bone was covered by a thick degenerated fibrous coat associated with fibroblasts, and the endosteum was adjacent to the bone marrow, which was occupied by multiple haemopoiesis tissue (Fig. 3i). Other results revealed that the bone tissue contained remnant lacunae of hyaline cartilage and a few osteocyte lacunae situated at the peripheral parts of bone tissue. The external aspect of bone tissue is adhered to by a thin strand of dense connective tissue; otherwise, the inner surface is surrounded by marrow cavities that have WBCs and RBCs (Fig. 3ii). The results of Masson's trichrome dyes showed extensive bone marrow associated with cellular debris, decrease in amount of collagen bundles, atrophy of lacunae, bulky blood vessels surrounded with vacuolated bone within the bone collar (Fig. 3iii).

The results of bone alteration in group 3 revealed a bony matrix with different sizes of lacunae. Moreover, there were atrophied osteocytes (Fig. 4). Other results showed longitudinal cracks situated within the bone matrix, which appeared devoid of any cellular elements and contained a few atrophied lacunae, several cavities within the bone matrix, one of them containing RBCs; the inner layer of the periosteum was devoid of osteoblasts (Fig. 4). Other spots showed a vesicular tunnel-like projection extending from the periosteum of bone to the bone matrix, with an increased number of atrophied lacunae; on the other hand, remnants of necrotic chondrocytes were demonstrated as dark lines (Fig. 4).

On the other hand, there is a decrease in the thickness of bone, collar with the appearance of multiple large cracks filled with necrotic cells; the other aspect of bone was devoid of periosteum. Figure 5 showed large cavities of future Haversian canals engorged with micro-vessels; the bone tissue was formed by a matrix associated with osteocytes. Other sections revealed immature collagen fibers within bone matrix, remnant of osteocytes within lacunae, formed vacuoles in the bone matrix containing cell debris, and irregular bone border devoid of endosteum. Remnants of collagen of bundles were scattered within bone matrix and there was a decreased amount of osteocytes (Fig. 5).

The results for group 4 in Figure 6i demonstrate that massive sinuses were present in the bony matrix, which are considered future Haversian canals with micro-blood vessels within it, adjacent to a scanty lacuna with osteocytes/atrophied, irregular aspect of bone devoid of a periosteal layer. Bone matrix contains many lacunae devoid of osteocytes and the bone aspect devoid of the fibrous layer coat of periosteum (Fig. 6ii). There was a degeneration in the fibrous layer of the periosteum and the bone lamellar matrix contained a significant lacuna with osteocytes formed within bone matrix (Fig. 6iii). Figures 6iv and 6v showed bone tissue that had many longitudinally eroded vacuoles with many lacunae devoid of osteocytes; in the periosteum, however, in some regions of bone, a few atrophied osteocytes appeared (Fig. 6vi). In Figures 6v and 6vi extensive cavities were present in the bony matrix with necrotic cellular elements, surrounded by many lacunae occupied by osteocytes. The cellular aspect of the inner periosteum was absent, and the outer aspect was just a delicate strand of collagen fiber.

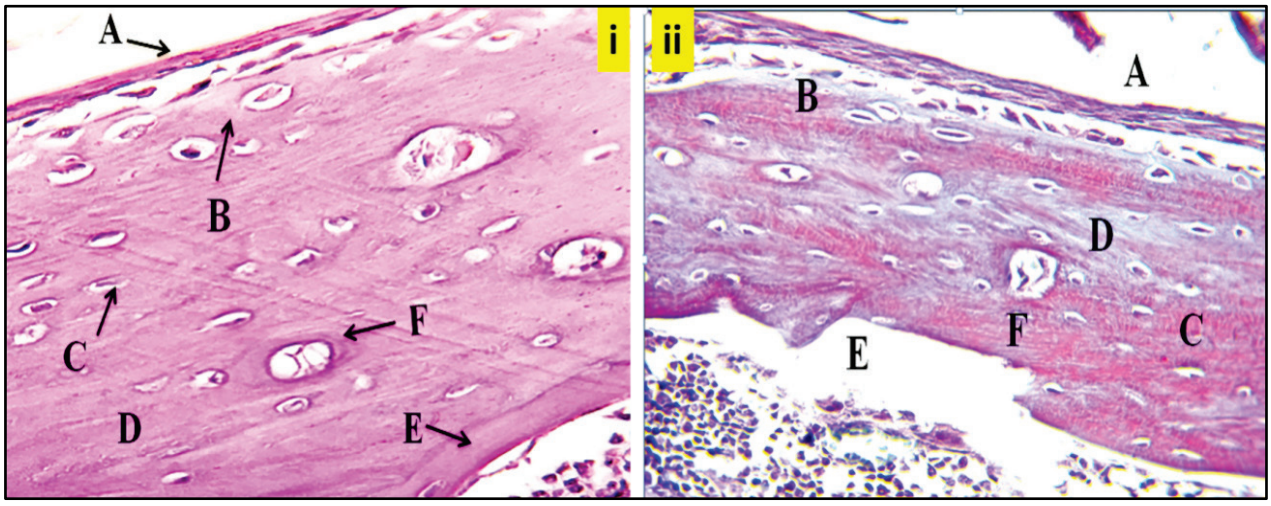

Fig. 1. Representative images for the femur bone of rabbits for the control group showing normal bone architecture: *A* – periosteum layer, *B* – osteoblast, *C* – osteocytes within lacunae, *D* – bony matrix, *E* – endosteum layer, *F* – Haversian canal; *i* – using hematoxylin and eosin, *ii* – using Masson's trichrome, 400X

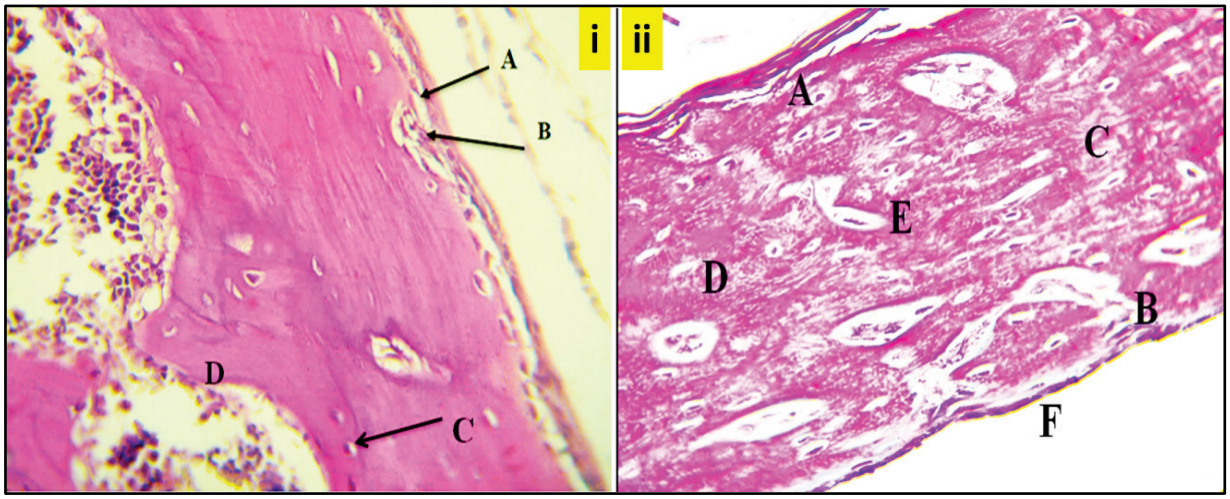

Fig. 2. Representative images for the femur bone of rabbits for the group 1: *i* showing *A* – periosteum, *B* – osteoblast, *C* – degeneration of osteocytes within lacunae, *D* – the irregular inner border of endosteum, using hematoxylin and eosin; *ii* showing *A* – periosteum devoid of osteogenic layer of, *B* – aggregate of cellular debris within sinus beneath endosteum, *C* – decrease in amount of collagen bundles, *D* – atrophy of osteocytes, *F* – endosteum with delicate connective tissue, using Masson's trichrome, 400X

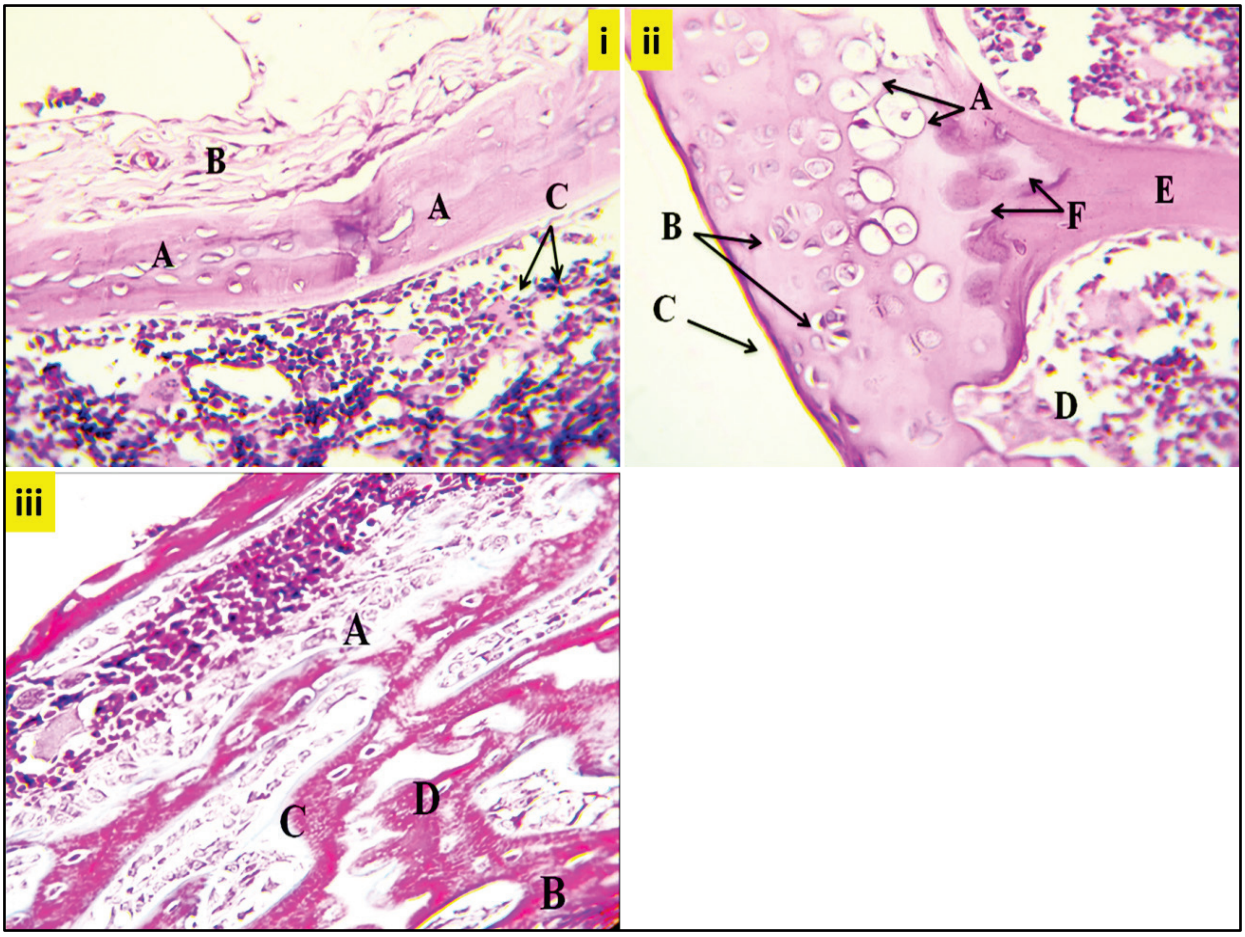

Fig. 3. Representative images for the femur bone of rabbits for the group 2: *i* showing *A* – bone collar devoid of osteocytes, *B* – thick fibrous coat with fibroblasts, *C* – bone marrow with cells, using hematoxylin and eosin; *ii* showing *A* – remnant chondrocytes, *B* – osteocytes with lacunae, *C* – dense connective tissue around the outer border of bone, *E* – bone spicule, *D* and *F* – marrow cells, using hematoxylin and eosin; *iii* showing *A* – extensive bone marrow associated with cellular debris, *B* – decrease in amount of collagen bundles, *C* – atrophy of lacunae, *D* – bulky blood vessels surrounded with cavitated bone collar, using Masson's trichrome, 400X

In Figure 7i, a necrotic area filled with necrotic elements in bone tissue underneath the necrotic fibrous layer of periosteum is surrounded by many lacunae with atrophied osteocytes. As demonstrated in Figure 7ii, the bony matrix had many vacuoles filled with necrotic elements; most of the bony lacunae were devoid of osteocytes; a few irregular bony lamellae were indicated, and the periosteal membrane was absent. Other sections showed a few scattered collagen bundles, with decreased osteocytes, longitudinal boney crack (Fig. 7iii). Other sections showed disappearance of fibrous layer of periosteum with atrophied osteogenic layer, degenerated collagen bundles, decrease of in number of osteocytes, irregular bone border, disorganization of degenerated collagen bundle and vacuolation within the bone collar (Fig. 7iv, 7v).

Discussion

Bone is a specialized mineralized connective tissue composed of many sympathetic and sensory nerve fibers. Osteogenesis is a significant biological process requiring cooperation of neurovascular supply, endocrine regulation, and many types of connective cells. Hormonal, autocrine, and paracrine processes control the modeling and remodeling of bone and neuronal pathways (Al-Suhaimi, 2022). The periosteum, bone marrow, and calcified bone all contain nerve fibers (Alencar et al., 2020). Botulinum toxin is used in numerous aspects of cosmetic surgery (Srivastava et al., 2015). The purpose of the current study was to evaluate the effect of paralyzed, flaccid skeletal muscles on the bones of femur albino rabbits.

The mechanism action of botulinum toxin B acts on neuro-muscular junctions which blocks release of acetylcholine neurotransmitter from the nerve fibers' endings and leads to flaccid paralysis. BoNT/B is used for treatment of cervical dystonia, hyperhidrosis and facial wrinkles (Raman et al., 2023). When botulinum toxin B was used in sialorrhea treatment, there was an increase in the incidence of xerostomia and dysphagia as side effects when compared with botulinum toxin A (Bomeli et al., 2008).

The results of the current study's histological investigation showed uneven endosteum surfaces. Outcomes of research by Ali et al. (2018) revealed several uneven, less acidophilic staining patches in the bone matrix. In some places, there were irregularly eroded patches on the endosteum aspect and osteocytes in the bone matrix; in others, the areas appeared degenerated, leaving large empty lacunae (Ali et al., 2018).

Histological examination in the present study revealed cleared lacunae from osteocytes and increased size of lacunae with atrophied osteocytes; Delgado demonstrated that the overdose medication of glucocorticoid and estrogen deficiency both enhanced the incidence of bone fragility disorders, or osteoporosis, in animal models and mechanical unloading, all of which are associated with a rise in osteocyte apoptosis (Ru & Wang 2020; Delgado-Calle & Bellido 2022). An alternative study showed that the bone matrix appeared devoid of any cellular elements and contained few atrophied lacunae; the rate of developed osteoblasts and the degree of apoptosis in osteoporosis both had an impact on the density of osteocytes (Gropp & Varela, 2024).

The current study's findings showed deteriorated periosteum, Gropp & Varela revealed that sensory nerve fibers connect osteoblasts and their progeny cells, osteoclasts, bone marrow cells, and endothelial layers of blood vessels by penetrating the inner layer of the periosteum next to the locations of the mineralized bony matrix (Gropp & Varela, 2024). Chen et al. showed the critical function that bone load plays in preventing osteoporosis; in the event of bone loss, this might be considered a means of compensating to maintain bone strength (Chen et al., 2008). On the other hand, results revealed shortened bone collars. The size of the fracture callus decreased at a more advanced stage of the healing process in limbs that were paralyzed (Nazzal et al., 2024; Tukeshov et al., 2024).

Other spots showed a vesicular tunnel-like projection extended from the periosteum of bone to the bone matrix, with an increased number of atrophied lacunae; on the other hand, remnants of necrotic chondrocytes were demonstrated as dark lines. This finding revealed the high level of demineralization of bone in the paralyzed limb. Dutra et al. (2018) suggested that the injection of BTX in the rat masseter muscle results in diminishing mineralization in the bony matrix and atrophied osteoclast cells.

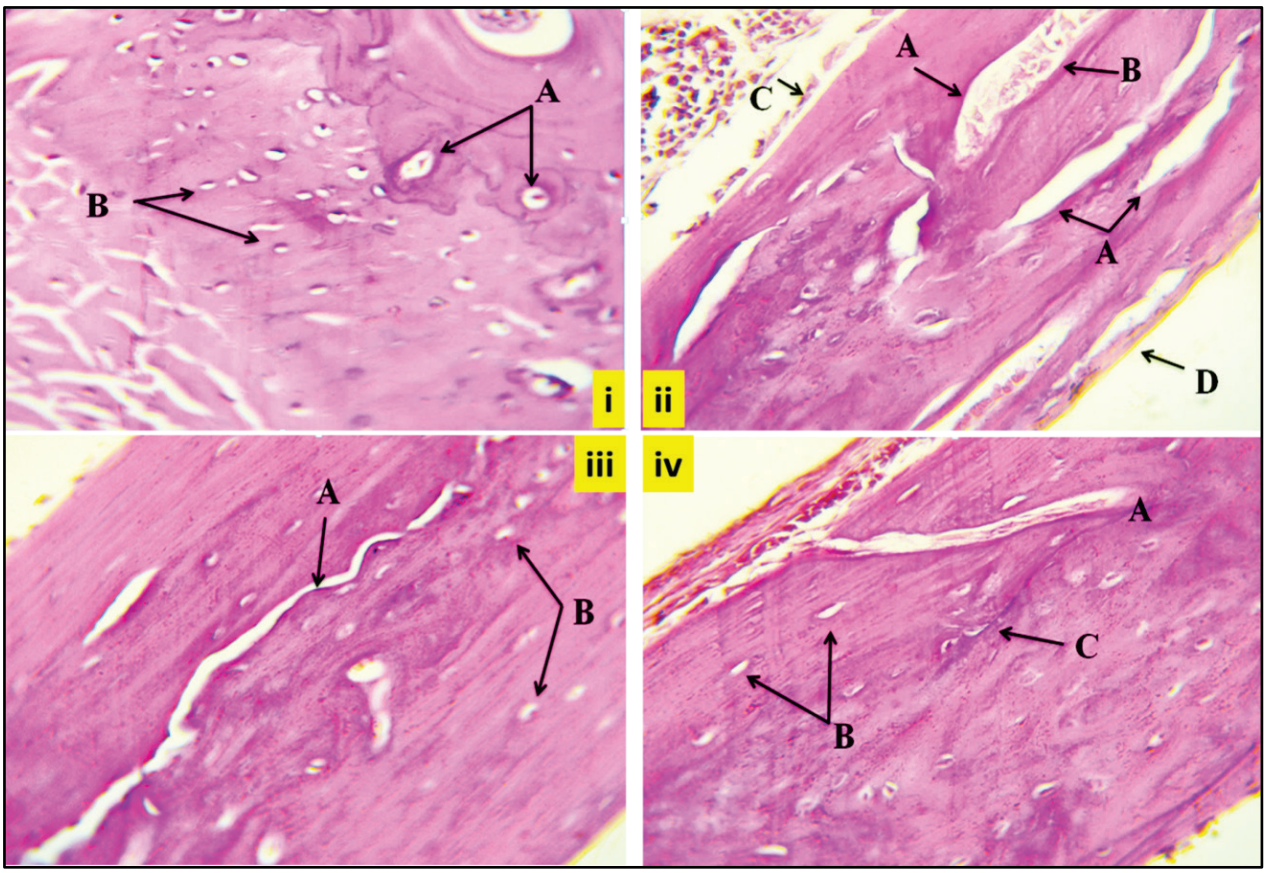

Fig. 4. Representative images for the femur bone matrix of rabbits for the group 3: *i* – showing *A* – bony matrix with different sizes of lacunae, *B* – atrophied osteocytes; *ii* showing *A* – longitudinal sinus and crack, *B* – filled up with RBCs, *C* – osteoblasts of the inner layer of endosteum, periosteum was devoid of osteogenic layer; *iii* showing *A* – longitudinal crack, *B* – atrophied osteocytes; *iv* showing *A* – bony matrix tunnel-like extension, *B* – lacunae with ill-defined osteocytes, *C* – remnant of necrotic chondrocytes, using hematoxylin and eosin, 400X

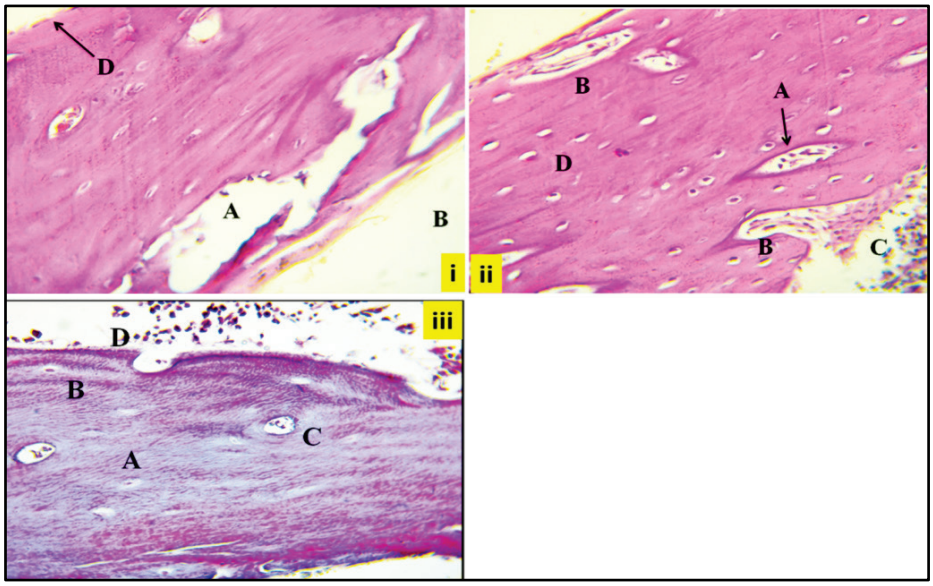

Fig. 5. Representative images for the femur bone cracks and cavities of rabbits for the group 3: *i* showing *A* – tremendous crack with necrotic cells, *B* – thin bone collar, *D* – bone devoid of periosteum, hematoxylin and eosin; *ii* showing *A* – bony matrix cavities with future Haversian canals, *B* – engorged with micro-blood vessels, *C* – bone marrow cells, *D* – osteocytes in lacunae, using hematoxylin and eosin; *iii* showing *A* – immature collagen fibers in bone matrix A, *B* – remnant of osteocytes within lacunae, *C* – formed vacuoles in the bone matrix containing cell debris, and irregular bone border devoid of endosteum, using Masson's trichrome, 400X

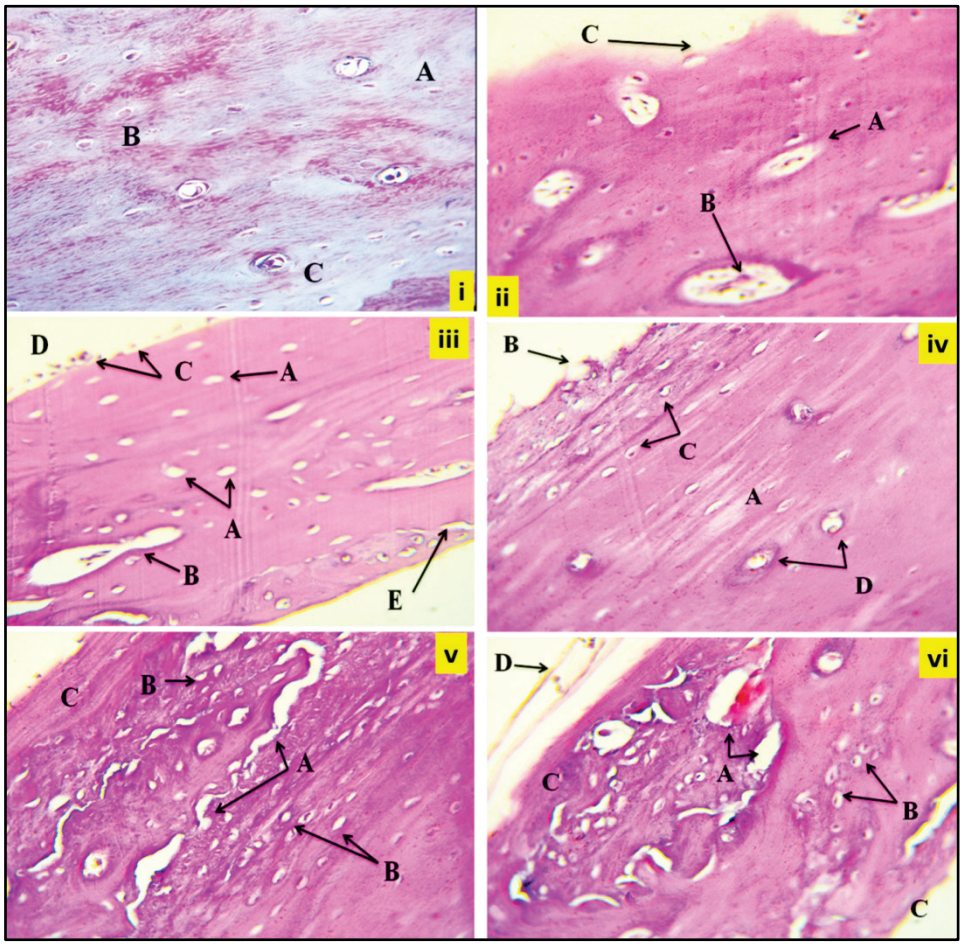

Fig. 6. Representative images for the femur bone matrix of rabbits for the group 4: *i* showing *A* – remnant sof collagen bundles were scattered within bone matrix, *B* – decrease of osteocytes, *C* – Haversian canal, using Masson's trichrome; *ii* showing *A* – massive sinus in a bony matrix with future Haversian canals, *B* – micro-vessels, *C* – irregular bone border devoid of periosteum, using hematoxylin and eosin; *iii* showing *A* – bony matrix with many lacunae devoid of osteocytes, *B* – Haversian canals, *C* – osteogenic layer devoid *D* – fibrous layer coat of periosteum, using hematoxylin and eosin; *iv* showing *A* – bony lamellae, *B* – degeneration in fibrous layer of periosteum, *C* – lacunae with osteocytes, *D* – significant lacunae, using hematoxylin and eosin; *v* showing *A* – longitudinal crack, *B* – lacunae without osteocytes, *C* – periosteum without osteogenic layer, using hematoxylin and eosin; *vi* showing *A* – eroded area, *B* – lacunae without osteocytes, *D* – periosteum devoid of osteogenic layer *C*, using hematoxylin and eosin, 400X

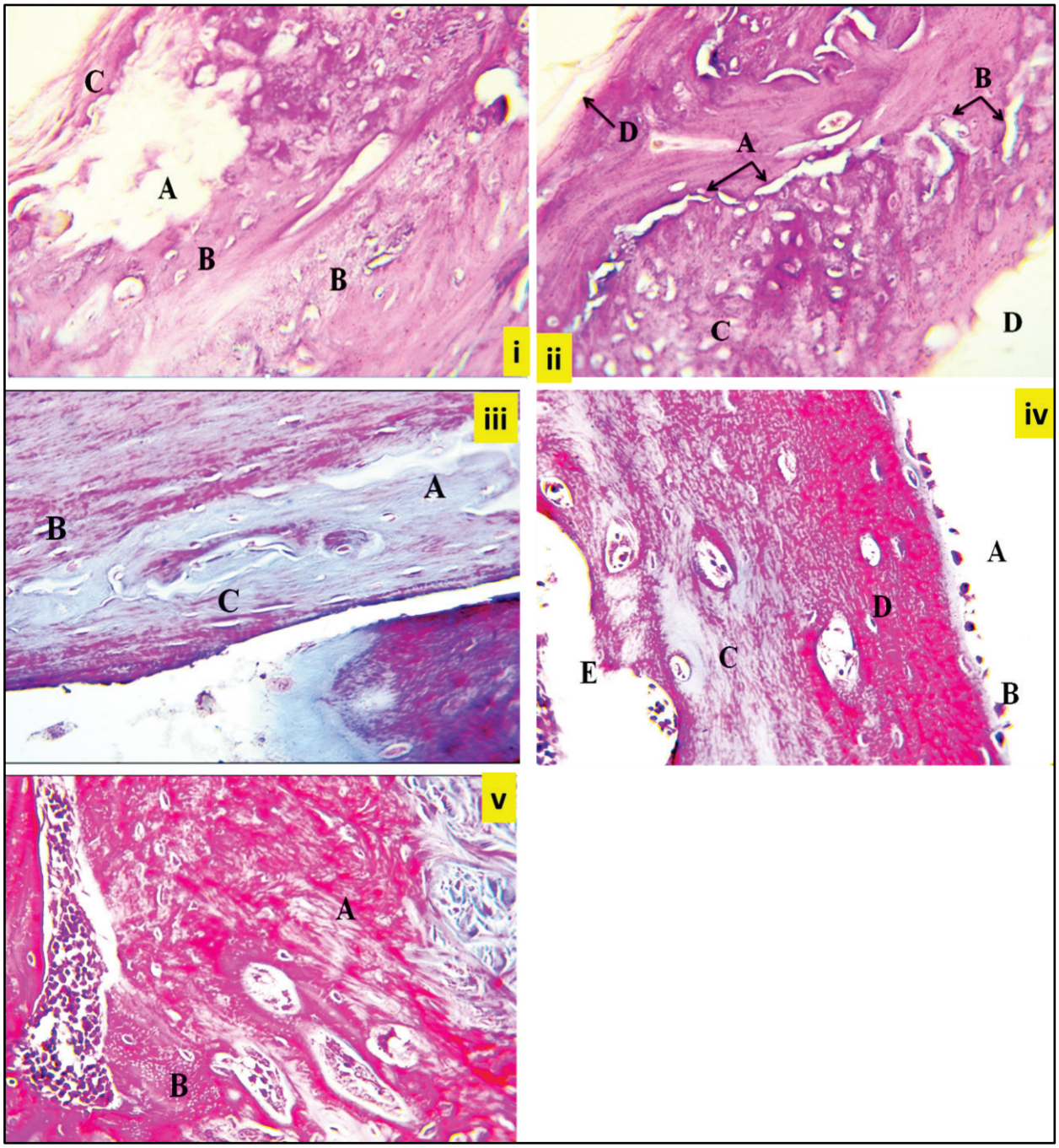

Fig. 7. Representative images of femur bone cracks and cavities in rabbits of the group 4: *i* showing *A* – necrotic cavity with cellular debris, *B* – atrophied osteocytes within lacunae, *C* – necrosis in fibrotic layer of periosteum, using hematoxylin and eosin; *ii* showing *A* – extensive cracks, with *B* – necrotic cellular debris, *C* – lacunae devoid of osteocytes, *D* – no signs of periosteal membrane, using hematoxylin and eosin; *iii* showing *A* – few scattered collagen of bundles, *B* – decrease of osteocytes, *C* – irregular bone crack, using Masson's trichrome; *iv* showing *A* – disappearance of fibrous layer of periosteum, *B* – atrophied osteogenic layer, *C* – degeneration of collagen bundles, *D* – decrease of osteocytes, *E* – irregular bone border, using Masson's trichrome; *v* showed *A* – disorganization of degenerated collagen bundle, *B* – vacuolation within bone collar, using Masson's trichrome, 400X

The group 4 results showed future Haversian canals, irregular bone aspects with diminishing periosteal membrane to endosteum, and necrotic areas filled with necrotic elements in bone tissue underneath degenerated periosteum. During the period that BTXA was injected into the fractured hind limb of a rat, fibro-calluses turned into an atrophied bone, with quadriceps muscle atrophy being the primary cause (Hao et al., 2012). In the present study, neurotoxin acted on the neuromuscular junction, leading to skeletal muscle atrophy and nerve injury blockers. Wua et al. (2021) revealed post-compressed sciatic nerve-induced forelimb muscle atrophy and decreased bone mass of the humerus and radius.

These results may be attributed to the mechanical forces of muscular bone which tightly induced the cytoplasmic membrane of osteocytes to convert into anti-apoptotic for osteocyte signals, which were mediated by the integrin protein pathway and focal adhesion kinases (FAKs) (Plotkin et al., 2005; Wawrzyniak & Balawender, 2022). Changes in circulating markers of bone metabolism indicate that early sciatic nerve damage, which impacts skeletal activity, stimulates bone resorption and lowers bone modeling activity (Taha et al., 2024). In the same group, microscopic examination showed large vacuoles filled with necrotic cells within the border of the bone; these results were consistent with the findings of Chappard et al. (2001) when employing botulinum toxin as a forelimb nerve blocker in rats: a decrease in the production of new bone, a quick rise in the resorption of existing bone because of a higher number of activated osteoclasts, and a perforation of the bone's longitudinally eroded area.

They result from the unloading of skeletal muscles (Chappard et al., 2001). Warner et al. (2006) investigated the impact of a large, unattended gap with osteocytes in most areas and a dispersed, uneven bone resorption caused by botulinum toxin. In the same experiments, Deng et al. (2021) suggested that both neurectomy and botox hind limb injection impaired osseointegration, which occurred in the cortical bone area. Takata & Yasui (2001) suggested that botulinum toxin-induced flaccid paralyzing of skeletal muscle (disuse) was accompanied by unbalanced bone remodeling in between bone resorption and bone modeling. These results agreed with the demonstrated results in the third and fourth groups, which showed numerous longitudinal cracks and erosion areas within the bone matrix. Botox inhibits the release of acetylcholine (ACH) neurotransmitters, leading to blocking nerve impulses. Therefore, the ACH level can contribute to bone protection, so botulinum toxin -induced bone osteoporosis changes.

The atrophied, irregular aspect of bone with a diminishing periosteal membrane to endosteum. Longitudinal Haversian canals were found. In Figure 7, the bone lamellar matrix contains a significant lacuna with osteocytes. The results obtained by Ali et al. (2018) showed multiple bone matrices with irregular, less acidophilic staining regions that were apparent. Irregular eroded areas were seen on the endosteum aspect and osteocytes in the bone matrix and were absent in some spots, while other spots appeared degenerated, leaving significant empty lacunae (Ali et al., 2018).

Other spots of the 4th group showed that the cellular aspect of the inner periosteum was absent, and the outer aspect was just a delicate strand of collagen fiber. Ali et al. (2018) revealed the atrophied periosteum, a remnant of necrotic tissue, which appeared as dark regions due to its extensive vascularity; the periosteum contains an abundance of pericytes. On the other hand, a necrotic area filled with necrotic elements in bone tissue underneath the degenerated periosteum is surrounded by many lacunae with atrophied osteocytes (Ravi et al., 2025). Pericytes are cells situated in contact with the capillary cell wall, and they can differentiate into various cell types, like osteoblasts (Zhu et al., 2022). Defective progenitor cells of blood vessels may affect adjacent cells such as osteocytes (Xu et al., 2024). Atrophied osteocytes will release numerous endogenous inflammatory cascades, induced osteoclast activity (Wang et al., 2022). The results of bone alteration revealed several cavities within the bone matrix, one of them containing RBCs; other results showed large cavities of future Haversian canals engorged with micro-vessels; the bone tissue was formed by a matrix associated with osteocytes, and beneath the outer aspect was invaded with blood vessels. Ashley et al. revealed that vascular changes result from the denervation of muscles, loss of contractile activity, and loss of muscular vascular pump activity. On the other hand, the denervation of vasoconstrictor blood vessels affects vascular tone and bone vascular blood flow (Ashley et al., 2007; Preethi et al., 2024).

Finally, the irregular endosteum showed a constricted bone collar with numerous lacunae, generally lacking osteocytes, decreased bone collar thickness, no periosteum, a significant split in the bony matrix, and irregular periosteum.

Conclusion

The femoral bone displayed numerous histological changes in this study due to the flaccid paralysis of the gluteal group muscles of the thigh caused by a single botulinum toxin B dose. These included an irregular endosteum, lacunae that were primarily devoid of osteocytes, large vacuoles, erosion cracks that appeared with cellular debris in the bony matrix, an irregular outer border of the bone with atrophied osteogenic cells, and an area of necrotic osteocytes within the bone matrix and fragments of bone. The bone defect was increased with prolonged periods of paralyzed skeletal muscles of the hind limb of albino rabbits.

References

Ahsanuddin, S., Roy, S., Nasser, W., Povolotskiy, R., & Paskhover, B. (2020). Adverse events associated with botox as reported in a food and drug administration database. Aesthetic Plastic Surgery, 45(3), 1201–1209.

Ajitha, R., Preethi, M., Sree, K. L., & Anbukkarasi, K. (2024). A histomorphological study of urinary bladder lesions in a tertiary care hospital. Texila International Journal of Public Health, 12(3), 48.

Al-Bari, A. A., & Al Mamun, A. (2020). Current advances in regulation of bone homeostasis. FASEB BioAdvances, 2(11), 668–679.

Alencar, C. H. M. F., Silveira, C. R. S., Cavalcante, M. M., Vieira, C. G. M., Teixeira, M. J. D., Neto, F. A., de Abreu, A., & Chhabra, A. (2020). Periosteum: An imaging review. European Journal of Radiology Open, 7, 100249.

Ali, D., Abdelzaher, W., & Abdel-Hafez, S. (2018). Evaluation of the rivastigmine role against botulinum toxin-A-induced osteoporosis in albino rats: A biochemical, histological, and immunohistochemical study. Human and Experimental Toxicology, 37(12), 1323–1335.

Ali, N. K. (2018). Estimation of some mineral (calcium, phosphorous, vitamin 25(OH) D, and alkaline phosphatase) in osteoporosis patients in Kirkuk city. Journal of Osteoporosis and Physical Activity, 6(2), 2–4.

Ali, S., Sulaiman, E., & Dhiaa, S. (2024). Histological effects of co enzyme Q_{10} on doxorubicin-induced deficits of cardiopulmonary axis in white albino rats. Georgian Medical News, (349), 54–59.

Alizadeh, A. M., Hashempour-Baltork, F., Alizadeh-Sani, M., Maleki, M., Azizi-Lalabad, M., & Khosravi-Darani, K. (2020). Inhibition of *Clostridium* (*C.*) *botulinum* and its toxins by probiotic bacteria and their metabolites: An update review. Quality Assurance and Safety of Crops and Foods, 12(SP1), 59–68.

Alkhafaji, N., Ahmed, M., & Karem, B. (2024). The effect of vitamin D on the histological structure of liver and lung in mice treated with amphotericin B. Georgian Medical News, (355), 134–141.

Al-Suhaimi, E. A. (2022). Bone remodeling physiology: Regulation of parathyroid glands, C cells, vitamin D, and bone as an endocrine organ. In: Al-Suhaimi, E. A. (Eds.). Emerging concepts in endocrine structure and functions. Springer Nature Singapore, Singapore. Pp. 161–199.

Ashley, Z., Sutherland, H., Lanmüller, H., Russold, M. F., Unger, E., Bijak, M., Mayr, W., Boncompagni, S., Protasi, F., Salmons, S., & Jarvis, J. C. (2007). Atrophy, but not necrosis, in rabbit skeletal muscle denervated for periods up to one year. American Journal of Physiology – Cell Physiology, 292(1), 440–451.

Atiyeh, B. S., Rubeiz, M. T., & Hayek, S. N. (2008). Aesthetic/cosmetic surgery and ethical challenges. Aesthetic Plastic Surgery, 44(4), 1364–1374.

Bartl, R. (2023). Secondary osteoporosis in medical disciplines. In: Bartl, R. (Ed.). Osteoporosis in clinical practice. Springer International Publishing, Cham. Pp. 165–187.

Bianco, P. (2020). Structure and mineralization of bone. In: Bonucci, E. (Ed.). Calcification in biological systems. CRC Press, Boca Raton. Pp. 243–268.

Bomeli, S. R., Desai, S. C., Johnson, J. T., & Walvekar, R. R. (2008). Management of salivary flow in head and neck cancer patients – A systematic review. Oral Oncology, 44(11), 1000–1008.

Brent, M. B., Brüel, A., & Thomsen, J. S. (2021). A systematic review of animal models of disuse – induced bone loss. Calcified Tissue International, 108(5), 561–575.

Brotto, M., & Bonewald, L. (2015). Bone and muscle: Interactions beyond mechanical. Bone, 80, 109–114.

Brown, A., & Teller, C. (2022). Identifying and managing complications caused by cosmetic neurotoxin treatment. Dermatological Reviews, 3(4), 247–256.

Carina, V., Della Bella, E., Costa, V., Bellavia, D., Veronesi, F., Cepollaro, S., Fini, M., & Giavaresi, G. (2020). Bone's response to mechanical loading in aging and osteoporosis: Molecular mechanisms. Calcified Tissue International, 107(4), 301–318.

Chappard, D., Chennebault, A., Moreau, M., Legrand, E., Audran, M., & Basle, M. F. (2001). Texture analysis of X-ray radiographs is a more reliable descriptor of bone loss than mineral content in a rat model of localized disuse induced by the *Clostridium botulinum* toxin. Bone, 28(1), 72–79.

Chen, H., Tian, X., Liu, X., Setterberg, R. B., Li, M., & Jee, W. S. S. (2008). Alfacalcidol-stimulated focal bone formation on the cancellous surface and increased bone formation on the periosteal surface of the lumbar vertebrae of adult female rats. Calcified Tissue International, 82(2), 127–136.

Delgado-Calle, J., & Bellido, T. (2022). The osteocyte as a signaling cell. Physiological Reviews, 102(1), 379–410.

Deng, J., Cohen, D. J., Redden, J., McClure, M. J., Boyan, B. D., & Schwartz, Z. (2021). Differential effects of neurectomy and botox-induced muscle paralysis on bone phenotype and titanium implant osseointegration. Bone, 153, 116145.

Devadze, R., Gvenetadze, A., Burkadze, G., & Kepuladze, S. (2022). Features of distribution of intratumoral lymphocytes in ovarian epithelial tumours of different histological types and degree of malignancy. Georgian Scientists, 4(5), 383–393.

Dutra, E. H., O' Brien, M. H., Lima, A., Kalajzic, Z., Tadinada, A., Nanda, R., & Yadav, S. (2016). Cellular and matrix response of the mandibular condylar cartilage to botulinum toxin. PLoS One, 11(10), e0164599.

Griffiths, D., & Mullock, A. (2017). Cosmetic surgery: Regulatory challenges in a global beauty market. Health Care Analysis, 26(3), 220–234.
Gropp, K. E., & Varela, A. (2024). Bones, joints, and teeth. In: Haschek, W. M., Rousseaux, C. G., ... & Bolon, B. (Eds.). Haschek and Rousseaux' s Handbook of toxicologic pathology. Academic Press. Pp. 249–360.
Hao, Y., Ma, Y., Wang, X., Jin, F., & Ge, S. (2011). Short-term muscle atrophy caused by botulinum toxin-A local injection impairs fracture healing in the rat femur. Journal of Orthopaedic Research, 30(4), 574–580.
Kelly, R. R., Sidles, S. J., & LaRue, A. C. (2020). Effects of neurological disorders on bone health. Frontiers in Psychology, 11, 612366.
Kim, H. J., Yum, K.-W., Lee, S.-S., Heo, M.-S., & Seo, K. (2003). Effects of botulinum toxin type A on bilateral masseteric hypertrophy evaluated with computed tomographic measurement. Dermatologic Surgery, 29(5), 484–489.
Kingery, W. (2003). A substance P receptor (NK1) antagonist enhances the widespread osteoporotic effects of sciatic nerve section. Bone, 33(6), 927–936.
Lanyon, L. E. (1996). Using functional loading to influence bone mass and architecture: objectives, mechanisms, and relationship with estrogen of the mechanically adaptive process in bone. Bone, 18(1), S37–S43.
Liu, S., Liu, S., Li, S., Liang, B., Han, X., Liang, Y., & Wei, X. (2023). Nerves within bone and their application in tissue engineering of bone regeneration. Frontiers in Neurology, 13, 1085560.
Nazzal, M. K., Morris, A. J., Parker, R. S., White, F. A., Natoli, R. M., Kacena, M. A., & Fehrenbacher, J. C. (2024). Do not lose your nerve, be callus: Insights into neural regulation of fracture healing. Current Osteoporosis Reports, 22(1), 182–192.
Nichat, P., Varadarajan, S., Balaji, T. M., Rao, N. N., Jayanandan, M., Govindarajan, S. (2024). Myofibroblasts and tumor micro-environment in oral squamous cell carcinomas – a histochemical and immunohistochemical analysis. Texila International Journal of Public Health, 12(3), 53.
Owen, M., Gray, B., Hack, N., Perez, L., Allard, R. J., & Hawkins, J. M. (2022). Impact of botulinum toxin injection into the masticatory muscles on mandibular bone: A systematic review. Journal of Oral Rehabilitation, 49(6), 644–653.
Park, M. Y., & Ahn, K. Y. (2021). Scientific review of the aesthetic uses of botulinum toxin type A. Archives of Craniofacial Surgery, 22(1), 1–10.
Plotkin, L. I., Mathov, I., Aguirre, J. I., Parfitt, A. M., Manolagas, S. C., & Bellido, T. (2005). Mechanical stimulation prevents osteocyte apoptosis: Requirement of integrins, Src kinases, and ERKs. American Journal of Physiology – Cell Physiology, 289(3), C633–C643.
Preethi, M., Roshan, A., Niranjan N., & Ajitha, R. (2024). A comparative study on rapid, simple and cost-effective method in determining the decalcification agent in bone tissue processing in hematoxylin and eosin staining procedure. Texila International Journal of Public Health, 12(3), 41.
Raman, S., Yamamoto, Y., Suzuki, Y., & Matsuka, Y. (2023). Mechanism and clinical use of botulinum neurotoxin in head and facial region. Journal of Prosthodontic Research, 67(4), 493–505.
Ravi, C., Manogaran, Y., & Ramasamy, P. (2025). Extraction, characterization and antioxidative potential of a bioactive polymeric material from the cuttlebone of *Sepia brevimana*. Texila International Journal of Public Health, 13(1), 69.
Ru, J., & Wang, Y. (2020). Osteocyte apoptosis: The roles and key molecular mechanisms in resorption-related bone diseases. Cell Death and Disease, 11(10), 846.
Srivastava, S., Kharbanda, S., Pal, U., & Shah, V. (2015). Applications of botulinum toxin in dentistry: A comprehensive review. National Journal of Maxillofacial Surgery, 6(2), 152–159.
Taha, M. M., Taha, E. M., & Mohammed, S. K. (2023). The role of testosterone level in women with osteopenia. Baghdad Science Journal, 21(2), 19.
Takata, S., & Yasui, N. (2001). Disuse osteoporosis. The Journal of Medical Investigation, 48(3–4), 147–156.
Tukeshov, S., Baysekeev, T., Choi, E., Kulushova, G., Nazir, M., Jaxymbayev, N., & Turkmenov, A. (2024). Osteosynthesis of complex comminuted hand bone fractures by applying the lacing method (a clinical case study). Georgian Medical News, 348, 40–43.
Vieira, A. E., Repeke, C. E., Ferreira Junior, S. de B., Colavite, P. M., Biguetti, C. C., Oliveira, R. C., Assis, G. F., Taga, R., Trombone, A. P. F., & Garlet, G. P. (2015). Intramembranous bone healing process subsequent to tooth extraction in mice: Micro-computed tomography, histomorphometric and molecular characterization. PLoS One, 10(5), e0128021.
Wang, P., Wang, C., Meng, H., Liu, G., Li, H., Gao, J., Tian, H., & Peng, J. (2022). The role of structural deterioration and biomechanical changes of the necrotic lesion in collapse mechanism of osteonecrosis of the femoral head. Orthopaedic Surgery, 14(5), 831–839.
Warner, S. E., Sanford, D. A., Becker, B. A., Bain, S. D., Srinivasan, S., & Gross, T. S. (2006). Botox induced muscle paralysis rapidly degrades bone. Bone, 38(2), 257–264.
Warner, S. E., Sanford, D. A., Becker, B. A., Bain, S. D., Srinivasan, S., & Gross, T. S. (2006). Botox induced muscle paralysis rapidly degrades bone. Bone, 38(2), 257–264.
Wawrzyniak, A., & Balawender, K. (2022). Structural and metabolic changes in bone. Animals, 12(15), 1946.
Wu, X., Xu, X., Liu, Q., Ding, J., Liu, J., Huang, Z., Huang, Z., Wu, X., Li, R., Yang, Z., Jiang, H., Liu, J., & Zhu, Q. (2021). Unilateral cervical spinal cord injury induces bone loss and metabolic changes in non-human primates (*Macaca fascicularis*). Journal of Orthopaedic Translation, 29, 113–122.
Xu, R., Li, S., Zheng, A., & He, L. (2024). Effect of Xiaoyao pills combined with alendronate on bone density in postmenopausal patients with osteoporosis. Georgian Medical News, 351, 100–101.
Yevchuk, Y., Rozhko, M., Pantus, A., Yarmoshuk, I., & Pantus, P. (2024). Analysis of the clinical effectiveness of using the created combined fibrin-bone scaffold for the reconstruction of bone tissue defects of the jaws. Georgian Medical News, 352–353, 6–13.
Zeng, Q. Q., Jee, W. S., Bigornia, A. E., King Jr., J. G., D'Souza, S. M., Li, X. J., Ma, Y. F., & Wechter, W. J. (1996). Time responses of cancellous and cortical bones to sciatic neurectomy in growing female rats. Bone, 19(1), 13–21.
Zhou, C., Zhang, W., Pang, W., Lin, H., Chen, M., & Wu, L. (2020). Dynamic changes of neuromuscular structure and function after local injection of botulinum toxin A. Revista Científica de la Facultad de Ciencias Veterinarias, 30(5), 2331–2341.
Zhu, S., Chen, M., Ying, Y., Wu, Q., Huang, Z., Ni, W., Wang, X., Xu, H., Bennett, S., Xiao, J., & Xu, J. (2022). Versatile subtypes of pericytes and their roles in spinal cord injury repair, bone development and repair. Bone Research, 10(1), 30.